Multisectoral climate impact hotspots in a warming world

Franziska Piontek[a,1], Christoph Müller[a], Thomas A. M. Pugh[b], Douglas B. Clark[c], Delphine Deryng[d], Joshua Elliott[e], Felipe de Jesus Colón González[f], Martina Flörke[g], Christian Folberth[h], Wietse Franssen[i], Katja Frieler[a], Andrew D. Friend[j], Simon N. Gosling[k], Deborah Hemming[l], Nikolay Khabarov[m], Hyungjun Kim[n], Mark R. Lomas[o], Yoshimitsu Masaki[p], Matthias Mengel[a], Andrew Morse[q], Kathleen Neumann[r,s], Kazuya Nishina[p], Sebastian Ostberg[a], Ryan Pavlick[t], Alex C. Ruane[u], Jacob Schewe[a], Erwin Schmid[v], Tobias Stacke[w], Qiuhong Tang[x], Zachary D. Tessler[y], Adrian M. Tompkins[f], Lila Warszawski[a], Dominik Wisser[z], and Hans Joachim Schellnhuber[a,aa]

[a]Potsdam Institute for Climate Impact Studies, Potsdam 14473 Germany; [b]Institute of Meteorology andClimate Research, Atmospheric and Environmental Research, Karlsruhe Institute of Technology, 82467 Garmisch-Partenkirchen, Germany; [c]Centre for Ecology and Hydrology, Wallingford OX1 08BB, United Kingdom; [d]School of Environmental Sciences, Tyndall Centre, University of East Anglia, Norwich NR4 7TJ, United Kingdom; [e]University of Chicago Computation Institute, Chicago, IL 60637; [f]Abdus Salam International Centre for Theoretical Physics, 34151 Trieste, Italy; [g]Center for Environmental Systems Research, University of Kassel, 34109 Kassel, Germany, [h]Swiss Federal Institute of Aquatic Science and Technology (EAWAG), 8600 Dübendorf, Switzerland; [i]Earth System Science, Wageningen University, 6708PB, Wageningen, The Netherlands; [j]Department of Geography, University of Cambridge, Cambridge CB2 1TN, United Kingdom; [k]School of Geography, University of Nottingham, Nottingham NG7 2RD, United Kingdom; [l]Met Office Hadley Centre, Exeter EX1 3PB, United Kingdom; [m]International Institute for Applied Systems Analysis, 2361 Laxenburg, Austria; [n]Institute of Industrial Science,University of Tokyo, Tokyo 153-8505, Japan; [o]Department of Animal and Plant Sciences, University of Sheffield, Sheffield S10 2TN, United Kingdom; [p]Center for Global Environmental Research, National Institute for Environmental Studies, Tsukuba 305-8506, Japan; [q]School of Environmental Sciences, University of Liverpool, Liverpool L69 3GP, United Kingdom; [r]PBL Netherlands Environmental Assessment Agency, 3720 AH, Bilthoven Wageningen University, 6700 AK, Wageningen, The Netherlands; [s]Rural Development Sociology, Wageningen University, 6706 KN Wageningen, The Netherlands; [t]Max Planck Institute for Biogeochemistry, 07745 Jena, Germany, [u]National Aeronautics and Space Administration Goddard Institute for Space Studies, New York, NY 10025; [v]Department for Economic and Social Sciences, University of Natural Resources and Life Sciences, 1180 Vienna, Austria, [w]Max Planck Institute for Meteorology, 20146 Hamburg, Germany, [x]Institute of Geographic Sciences and Natural Resources Research, Chinese Academy of Sciences, Beijing 100101, China, [y]City University of New York Environmental Cross-Roads Initiative, City College of New York, New York, NY 10031; [z]Department of Physical Geography, Utrecht University, 3508 TC Utrecht, The Netherlands; and [aa]Santa Fe Institute, Santa Fe, NM 87501

Edited by Robert W. Kates, Independent Scholar, Trenton, ME, and approved June 4, 2013 (received for review January 31, 2013)

The impacts of global climate change on different aspects of humanity's diverse life-support systems are complex and often difficult to predict. To facilitate policy decisions on mitigation and adaptation strategies, it is necessary to understand, quantify, and synthesize these climate-change impacts, taking into account their uncertainties. Crucial to these decisions is an understanding of how impacts in different sectors overlap, as overlapping impacts increase exposure, lead to interactions of impacts, and are likely to raise adaptation pressure. As a first step we develop herein a framework to study coinciding impacts and identify regional exposure hotspots. This framework can then be used as a starting point for regional case studies on vulnerability and multifaceted adaptation strategies. We consider impacts related to water, agriculture, ecosystems, and malaria at different levels of global warming. Multisectoral overlap starts to be seen robustly at a mean global warming of 3 °C above the 1980–2010 mean, with 11% of the world population subject to severe impacts in at least two of the four impact sectors at 4 °C. Despite these general conclusions, we find that uncertainty arising from the impact models is considerable, and larger than that from the climate models. In a low probability-high impact worst-case assessment, almost the whole inhabited world is at risk for multisectoral pressures. Hence, there is a pressing need for an increased research effort to develop a more comprehensive understanding of impacts, as well as for the development of policy measures under existing uncertainty.

coinciding pressures | differential climate impacts | ISI-MIP

Over the coming decades, climate change is likely to significantly alter human and biological systems, pushing the boundaries of variability beyond historic values and leading to significant changes to what are considered typical conditions. Identifying the locations, timings, and features of these impacts for a given level of global warming in advance allows the development of appropriate adaptation strategies, or can motivate decisions to mitigate climate change. Although climate-change impacts are extensively studied in individual sectors, their overlaps and interactions are rarely taken into account. However, these impacts are likely to be of great consequence, as they can amplify effects, restrict response options, and lead to indirect impacts in other regions, thus strongly increasing the challenges to adaptation (1). In this article we take an important first step toward the analysis of these effects through a consistent assessment of the geographical coincidence of impacts as multisectoral exposure hotspots. The Intersectoral Impact Model Intercomparison Project (ISI-MIP, www.isi-mip.org) offers a unique opportunity for this analysis by providing multimodel ensembles of climate-change impacts across different sectors in a consistent scenario framework.

Through the investigation of biophysical impacts of climate change, which form the linkage between climate and society (2, 3), this study moves beyond previous hotspot analyses that have mostly used purely climatic indicators (4–7). In addition, the setup enables an assessment of uncertainty because of both multiple Global Climate Models (GCMs) and multiple Global Impact Models (GIMs) in each sector (8). Finally, impacts are analyzed at different levels of global mean temperature (GMT) for a comparison at different levels of global warming. This global analysis serves two objectives. First, tangible adaptation strategies require knowledge of local vulnerability, defined by exposure, sensitivity, and adaptive capacity. The regional exposure hotspots can therefore serve as a starting point for prioritized case studies and studies of interactions as the basis for the development of adaptation strategies that can be expanded to additional regions as needed. Second, the focus on GMT change is crucial when studying costs and benefits of mitigation policies,

Author contributions: F.P., K.F., J.S., L.W., and H.J.S. designed research; F.P. performed research; F.P., C.M., T.A.M.P., D.B.C., D.D., J.E., F.d.J.C.G., M.F., C.F., W.F., A.D.F., S.N.G., D.H., N.K., H.K., M.R.L., Y.M., M.M., A.M., K. Neumann, K. Nishina, S.O., R.P., A.C.R., E.S., T.S., Q.T., Z.D.T., A.M.T., and D.W. analyzed data; and F.P., C.M., and T.A.M.P. wrote the paper.

The authors declare no conflict of interest.

This article is a PNAS Direct Submission.

[1]To whom correspondence should be addressed. E-mail: piontek@pik-potsdam.de.

This article contains supporting information online at www.pnas.org/lookup/suppl/doi:10.1073/pnas.1222471110/-/DCSupplemental.

such as the 2 °C target set by the international community to reduce risks from climate-change impacts and damages (9, 10).

The analysis comprises four key impact sectors: water, agriculture, ecosystems, and health. Health is represented by malaria (albeit, there is only one example of health impacts of climate change), which does have potentially severe economic consequences (11). As metrics for the four sectors, we select river discharge as a measure of water availability, crop yields for four major staple crops (wheat, rice, soy, and maize) on currently rain-fed and irrigated cropland (12) (Fig. S1), the ecosystem change metric Γ (13), and the length of transmission season (LTS) for malaria. Although these four metrics do not cover the full range of possible societally relevant climate-change impacts, they do include crucial aspects of livelihoods and natural resources, especially for developing countries: water availability, food security, ecosystem stability, and a key health threat.

We aim to define levels of change in each sector that can be considered severe as basis for multisectoral hotspots. "Severe" is taken to mean a shift of average conditions across selected thresholds representing significant changes relative to the historical norm. A multisectoral perspective is thus possible through the simultaneous occurrence of above-threshold changes in multiple sectors. Although climate change can have both positive and negative impacts, for the purpose of vulnerability analysis we identify hotspots of changes that put additional stresses on human and biological systems. Average conditions are measured as the median over 31-y time periods. For the thresholds, we take a statistical approach for water availability and crop yields, whereas we use a more comprehensive metric for ecosystem change, and resort to a relatively simple indicator for malaria conditions. The thresholds in the water and agricultural sectors are defined as the 10th percentile of the reference period distribution (1980–2010) of discharge and crop yields, respectively. This threshold means a shift of average conditions into what is considered today moderately extreme, happening in only 10% of all years. Behavior is robust to the choice of a smaller threshold (Fig. S2). This low end of the distribution excludes floods, as the focus is on reduced water availability. Clearly, the chance to cross the threshold depends on the level of variability in a given region and may in fact mean relatively small absolute change; however, it reflects the assumption that people in regions already subject to highly variable conditions are better prepared to adapt to more extreme average conditions (14).

The Γ-metric (13) represents the difference between future states of ecosystems and present day conditions through an aggregate measure of changes in stores and fluxes of carbon and water, as well as vegetation structures. A large value of Γ indicates significant changes in biogeochemical conditions or vegetation structure, which would likely lead to considerable transformations of the ecosystem. Based on differences between present day ecosystems, Heyder et al. (13) define $\Gamma > 0.3$ as the threshold for a risk of severe change, [see also Warszawski et al., (15)]. Such changes may reduce biodiversity, which is crucial for the resilience of many ecosystem services (16). Furthermore, the livelihoods of many vulnerable populations, along with cultural values and traditions, are closely tied to existing ecosystems (17). The threshold for changes in the prevalence of malaria is defined as a shift in the LTS, from < 3 mo to >3 mo. This shift corresponds approximately to a switch from epidemic to endemic malaria based on climatic conditions (based on data from the Mapping Malaria Risk in Africa project, www.mara.org.za) (Fig. S3).

All impacts are simulated with multiple, predominantly process-based GIMs (agriculture and ecosystems, 7 models each; water, 11 models; malaria, 4 models). These GIMs are driven by three GCMs, simulating the highest representative concentration pathway (RCP8.5) (18). Although current emissions are following a similar trajectory, we choose RCP8.5 primarily to cover the largest possible temperature range, not as a worst-case scenario (19). For each GIM-GCM combination and at each grid point, we define a "crossing temperature" that is the GMT change (ΔGMT) at which the sectoral metric crosses the respective impact threshold. Sectoral crossing temperatures are then taken as the median over all GIM-GCM combinations of a given sector. In our strict assessment, only robust results are taken into account, defined as an agreement of at least 50% of all GIM-GCM combinations of a given sector at which the threshold is crossed. Overlapping pressures at a given grid point are assumed to arise when multiple sectors have crossed at a given ΔGMT. Results are presented in terms of total area affected by the shift as a function of ΔGMT. Note that GMT changes in this report are with respect to the 1980–2010 period, which is ∼0.7 °C above preindustrial levels (20).

Results and Discussion

Sectoral Analysis. The basis for the study of multisectoral overlap is the ΔGMT level at which the thresholds for severe change are crossed (if at all) in each of the four sectors (Fig. 1 and Fig. S4). Median 31-y water availability is projected to drop below the reference distribution's 10th percentile in the Mediterranean, regions of South America, in particular the southern Amazon basin, regions in coastal western and central Africa, and parts of south-central Asia for a warming of up to 4.5 °C under RCP8.5. This distribution includes some regions of large projected relative drop in discharge (21), although the relatively strict 10th percentile criterion means that it does not capture all of them (e.g., southern United States). The regions affected by crop yields below the threshold are tropical regions dominated by rain-fed agriculture; this is consistent with the expectation that rain-fed systems are likely to see larger and more consistent yield losses than irrigated areas that can adapt more successfully. No negative effects on yields are seen at higher latitudes, as these initially benefit from higher temperatures and CO_2 fertilization effects and exhibit yield increases (22, 23). For both discharge and yields, thresholds start to be crossed at ΔGMT = 1 °C.

Significant risk of ecosystem change, as indicated by the Γ-metric, has the largest geographical extent of all sectors, with most regions exhibiting crossing temperatures of 3–4 °C. This large extent occurs because it encompasses very different ecosystem responses. There is forest die-back because of less rainfall in the Amazon and heat stress in boreal forest regions, but also increased greening in Europe and Africa because of warmer, wetter conditions, as well as replacement of some vegetation species with others better adapted to the new conditions. Forest advances northward as a result of higher temperatures and the trees' increased water-use efficiency in response to higher atmospheric CO_2 concentrations. On the Tibetan Plateau, distinguished by the lowest crossing temperature of ΔGMT = 2 °C, increased vegetation growth because of longer growing seasons and warmer winters puts the current grass and shrublands at risk. Although not all of these changes will be negative per se, they would constitute a disruption and possibly a need for adaptation of local societies to the prevailing ecosystem conditions.

Finally, malaria prevalence is expected to increase in higher latitudes, higher altitudes, and in regions on the fringes of current malaria regions because of warmer and wetter climatic conditions. However, when conditions become drier, prevalence can also decrease. As a result of the very different parameterizations used in the four malaria models considered here, agreement among models on the changes is poor, leaving very few areas as robustly crossing the 3-mo LTS threshold. Nevertheless, in agreement with previous work, the Ethiopian Highlands are one of these regions (24, 25).

Multisectoral Hotspots. We define hotspots as regions of multisectoral exposure where two or more of the sectoral metrics have crossed their respective thresholds of severe change in average

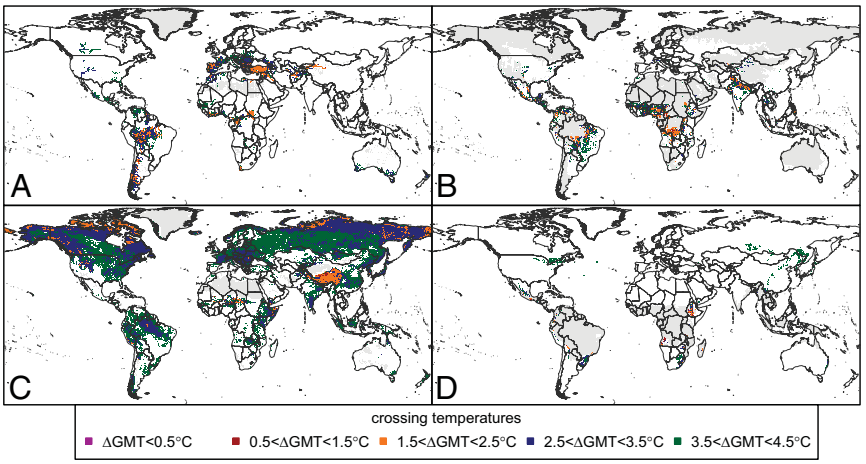

Fig. 1. Threshold crossing temperatures with respect to the reference period GMT for the four sectoral metrics: discharge (*A*), crop yields (*B*), risk of severe ecosystem change (*C*), and LTS of malaria (*D*). Areas in white do not cross the respective threshold. The gray color indicates regions which are either masked out [discharge, Γ, crop yields (only regions where the maize, wheat, soy, and rice are currently cultivated are considered)], or where malaria is already endemic (*D*). An agreement of 50% of all GIM-GCM combinations on threshold crossing is required for consideration in the analysis.

conditions under the strict assessment, which means with high likelihood (Fig. 2). According to our results there is no overlap of severe change in all four sectors. The most prominent hotspot is the southern Amazon basin, with some parts projected to experience severe changes in three sectors (yields, ecosystems, and discharge) and large areas affected by two pressures. The second largest hotspot region is southern Europe, with overlapping changes in discharge and ecosystems. These two areas, as well as smaller tropical hotspot regions in Central America and Africa, were also identified in other studies using different methods, supporting our findings (5, 6). In addition, we identify the Ethiopian highlands as a hotspot because of the overlap of malaria extension, crop yield reduction, and ecosystem change; northern regions of south Asia are affected by either reductions in discharge and crop yields or crop yield reduction and ecosystem change. These multisectoral hotspots occur in both regions with high population density (i.e., Europe, east Africa, south Asia) and sparsely populated areas (i.e., Amazon). These hotspots cover developed, emerging, and developing economies, each with different degrees of adaptive capacity and sensitivity to the multisectoral pressures. Note that these factors are not taken into account here. A weighting of the relative importance of the sectoral pressures depends strongly on local factors, such as societal structures and values, economic base, and environmental imperatives. Therefore, a more detailed interpretation of the hotspots requires in-depth regional case studies, but is beyond the scope of this study.

Regions typically expected as high-exposure regions, like Africa, do not emerge strongly as hotspots here, which is partially because of the sectors used in the analysis and the individual characteristics of the sectoral metrics, both influencing their combination. In particular, the global area where three or four regions can potentially overlap is limited to where the four staple crops are currently cultivated and where malaria is not yet endemic (excluding gray areas in Fig.1). Hence, a different picture might arise if, for example, changes in the occurrence of extreme events, like droughts and floods, were included as metrics, which would likely increase the occurrence of hotspots in Africa and south-east Asia (26).

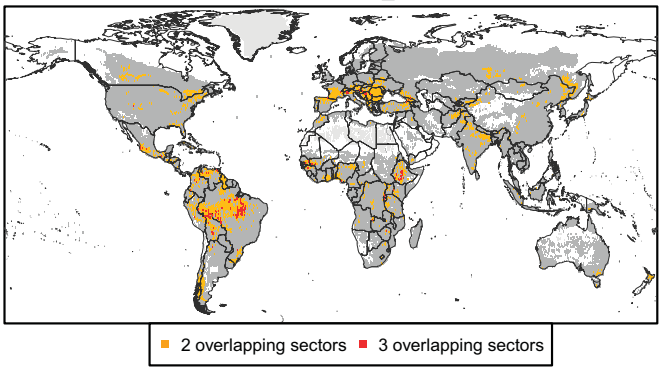

Fig. 2. Multisectoral hotspots of impacts for two (orange) and three (red) overlapping sectors in the strict assessment, with 50% of GIM-GCM combinations agreeing on the threshold crossing in each sector, for a GMT change of up to 4.5 °C. Which sectors overlap depends on the location and can be discerned from the sectoral patterns in Fig.1. An overlap of all four sectors does not occur in the strict assessment. Regions in light gray are regions where no multisectoral overlap is possible at all because of sectoral restrictions as shown in Fig.1. The dark gray shows the additional regions affected by multisectoral pressures under the worst-case assessment, where a minimum of 10% of all sectoral GIM-GCM combinations have to agree on the threshold crossing.

The Role of Uncertainty. An additional factor limiting the overlap of areas with severe change in different sectors is the large uncertainty in projections, stemming mainly from the GCMs and GIMs. When the results for the three GCMs are separated, different multisectoral hotspot patterns emerge, with some regions only appearing as hotspots with a single GCM (Fig. S5). This appearance is because of different sectoral patterns associated with each GCM as a result of variances in projections of key climate variables influencing the impact models. Climate model uncertainty is therefore an important cause of the limited sectoral overlap in our analysis. Uncertainty from impact models, however, is much larger (Fig. 3 and Fig. S2). This finding is in agreement with previous literature and other analyses in this Special Features issue of PNAS (15, 21, 27, 28). Agreement is highest among the ecosystem models, whereas differences are largest between the global crop models. In addition to uncertainty as to whether the thresholds are crossed, there is also uncertainty on the crossing temperature, with SDs of around 1 °C in most sectors (Fig. S6). The details of the model differences are beyond the scope of this report. However, we emphasize the importance of accompanying this study with detailed sectoral

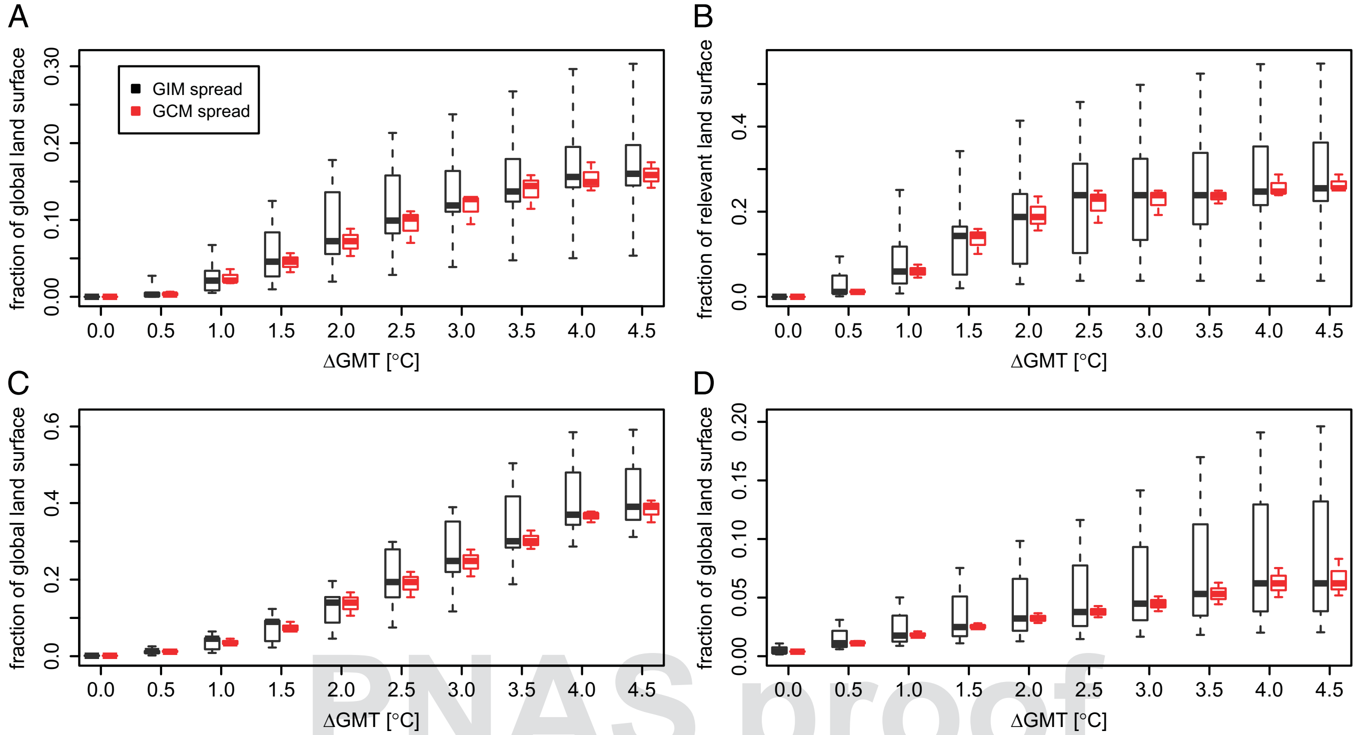

Fig. 3. Cumulative fraction of global land area (excluding Antarctica; for crop yields the relevant area is the maximum crop area as covered today by the four staple crops: maize, wheat, soy, and rice) having crossed the respective sectoral thresholds up to the given ΔGMT for discharge (*A*), crop yields (*B*), risk of severe ecosystem changes (*C*), and LTS (*D*). Black boxes show the uncertainty across impact models, and red boxes indicate the uncertainty across GCMs. Each box indicates the interquartile range, the thick line shows the median, and the whiskers extend over the whole range of the distribution of all GCMs/GIMs at that temperature bin. Note the different ranges on the *y* axis for each panel.

understanding and analysis, which can be found elsewhere in this issue (see also *SI Text*) (15, 21, 22, 24).

This high level of uncertainty warrants the strict robustness limit of 50% agreement among GIM-GCM combinations used for the identification of hotspots. At the same time, this uncertainty may mask a remaining risk, given that models appearing at the ends of the distribution cannot be disregarded because no performance-weighting of models was carried out. Therefore, we also provide a worst-case assessment of multisectoral hotspots, with crossing temperatures determined as the 10th percentile of all crossing temperatures in a given grid cell. This process means that only 10% of all GIM-GCM combinations have to agree on the threshold crossing (chosen to have at least two in a sector, to avoid spurious effects of one outlier) and the resulting crossing temperatures are lower limits. This worst-case assessment shows a large additional extent of multisectoral overlap (Fig. 2, dark gray areas) with almost all of the world's inhabited areas affected. The areas with highest exposure in this case have an overlap of all four sectors (Fig. 3 and Fig. S7). This worst case is rather extreme, but nonetheless it represents the upper end of the risk spectrum in light of the large uncertainties.

Aggregate Effects with GMT. The total global area and population that are projected to face average conditions that are considered rare today in more than one sector increases with GMT (Fig. 4). The likelihood for multisectoral overlap increases with the area

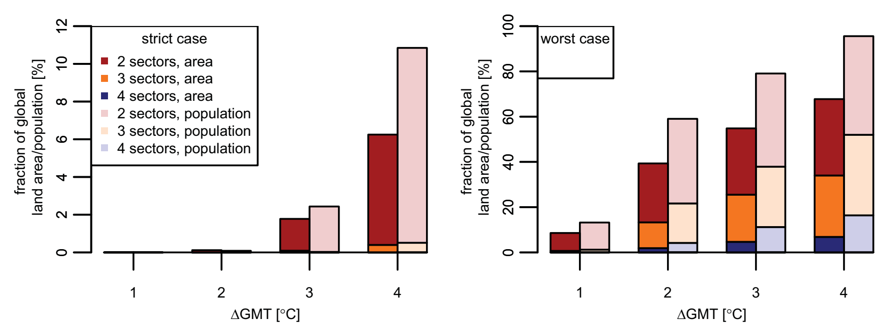

Fig. 4. Cumulative fraction of the global area (brightly tinted bars, excluding Antarctica) and population (lightly tinted bars) affected by the thresholds being crossed at ΔGMT in at least two (red), three (orange), and four (blue) overlapping sectors. (*Left*) The strict case (agreement of at least 50% of GIM-GCM combinations on the threshold crossing). (*Right*) The worst-case (agreement of at least 10% of GIM-GCM combinations on the threshold crossing and the sectoral crossing temperature is the 10th percentile of all crossing temperatures) assessment. Overlap of four sectors does not occur in the strict case. Population is held constant at the year 2000 levels.

affected in the individual sectors, one reason for the onset of multisectoral pressures at relatively high levels of GMT change only. For the strict assessment, multisectoral severe pressure begins at ΔGMT = 3 °C above the 1980–2010 baseline; at 4 °C roughly 6% of the global area (excluding Antarctica) and close to 11% of the global population are affected. Correspondingly, the largest increases in the areas having crossed the thresholds in each sector are seen between ΔGMT = 1 °C and 3 °C (Fig. 3), with some indications for saturation after that. Further increases in affected areas are possible at higher ΔGMT levels than studied here. For example, a peak and possible later decline in crop yields is expected as a result of heat stress overtaking the initial benefits of the CO_2 fertilization effect.

In the worst-case analysis, area and population affected is already much larger at lower levels of ΔGMT, with the largest increase between 1 °C and 2 °C above the 1980–2010 baseline and an inflection of the trend after that. Almost the entire global population is exposed to multisectoral pressure at ΔGMT = 4 °C. In addition, roughly 18% of the global population is projected to experience severe pressure in all four sectors. The affected regions are in Europe, North America, and south-east Asia (Fig. S7), driven by the extension of malaria prevalence to higher latitudes. This interpretation may give too much emphasis to this pressure, as malaria distribution also depends strongly on socioeconomic factors but is here only driven by climate suitability (29). Nevertheless, the increased overlap of three or even four sectors in the worst-case assessment indicates a strong adaptation pressure, albeit at low probability.

Implications and Further Research

This identification of multisectoral hotspots of climate change impacts is to our knowledge unique in its use of a consistent framework with multiple impact models per sector and using ΔGMT as a metric for climate change. Our global analysis provides a starting point for more detailed understanding of the extended implications of climate change for exposure and adaptation actions. Although geographically overlapping impacts only start at ΔGMT = 3 °C above the 1980–2010 baseline (almost 4 °C above preindustrial GMT levels), large increases in exposed areas within the sectors start at around 2.2 °C above preindustrial levels. In the worst-case analysis, the largest increase in affected area and population occurs between roughly 2 °C and 3 °C above preindustrial levels. This finding provides important insight for mitigation strategies.

The identified multisectoral hotspots are geographically diverse, including the southern Amazon basin, southern Europe, the Ethiopian highlands, and northern India, and are driven by different combinations of coinciding sectors. Implications and possible feedbacks between the overlapping sectors can be investigated in regional case studies. At the same time, these hotspots could affect distant regions through indirect effects, such as trade or migration. Appropriate adaptation planning that considers coinciding (and also interacting) pressures facilitates the development of strategies designed to address such multiple challenges, and avoids creating solutions for one pressure that possibly seriously exacerbates another (e.g., draining wetlands to reduce malaria in an area prone to increases in flooding).

The set-up for our analysis explicitly includes uncertainty in both climate and impact models. This format shows that uncertainties from both GIMs and GCMs are large, limiting the robustness of the conclusions; however, it should not hamper action at this point, as some level of uncertainty will always be present. In particular the low probability-high impact worst-case assessment, which shows a very large extent of multisectoral pressures starting at lower temperature changes, provides a strong motivation for more detailed impacts research.

Because it is unique, our analysis is a methodological experiment, to be refined in the light of experience. Indeed, different patterns may emerge if different sectors or absolute magnitudes of change are included. A comparison of hotspots generated with different methodologies will provide valuable insights into impact dynamics. The identification of hotspots of positive climate-change impacts would create a more balanced and comprehensive picture, but requires different metrics to those used here. In addition, although a simple overlap of the different sectoral metrics is considered here, the challenge for future analyses is also to integrate the interactions between the different sectors and indirect effects over large distances, which may alter the spatial pattern of hotspots. Examples are interactions between water availability and irrigation or ecosystem services, and irrigation and malaria occurrence (28, 30). Furthermore, a more comprehensive understanding of human vulnerability hotspots requires a thorough analysis, combining highly resolved indicators of adaptive capacity and sensitivity (which so far seem to be lacking) with biophysical hotspot indicators as measures of exposure (2, 3). Nevertheless, our study is an important step toward a consistent integration of multiple sectors in impacts research, and identifies the risk of sizable hotspots of multisectoral pressures under highly plausible levels of global warming.

Materials and Methods

Models and Data. For this analysis, simulations were driven by the three ISI-MIP GCMs that exhibit a ΔGMT= 4 °C by the end of the 21st century (HadGEM2-ES, MIROC-ESM-CHEM, IPSL-CM5A-LR). To improve statistical agreement with observations, a bias correction was applied to the climate data. This bias constitutes an additional source of uncertainty and reduces the spread of present-day GCM climatologies (31–34). The gridded year 2000 population data are based on United Nations World Populations Prospects data, scaled to match the country totals of the new Shared Socio-Economic Pathway population projections for the middle-of-the-road case (SSP2; https://secure.iiasa.ac.at/web-apps/ene/SspDb) using the National Aeronautics and Space Administration GPWv3 y-2010 (http://sedac.ciesin.columbia.edu/data/collection/gpw-v3) gridded population dataset (35, 36). Similar results for the percentage of affected global population are found when the projected values for 2084 are used (Fig. S8). Impacts were simulated on terrestrial pixels of a global 0.5° mesh (roughly 55 km wide at the equator). For an overview of the GIMs used in the analysis, see Tables S1–S4, accompanied by a brief discussion of model differences contributing to the spread in results. The global gridded crop model intercomparison was coordinated by the Agricultural Model Intercomparsion and Improvement Project (37).

Impact Metrics. All metrics have annual temporal resolution, neglecting seasonal patterns. To avoid spurious effects, values are set to zero below the lower limits 0.01 $km^3 \cdot yr^{-1}$ and 2.5% natural vegetation cover, for discharge and ecosystem change, respectively (15, 38). The four crops are combined by converting to energy-weighted production per cell using the following conversion factors for energy content (MJ kg^{-1} dry matter): wheat (spring/winter), 15.88; rice (paddy), 13.47; maize, 16.93; soy, 15.4 (39, 40). The extent of potential agricultural hotspots is limited; for example, millet and sorghum, which are widely grown in Africa, are not included in the analysis. The impact of climate change on malaria occurrence focuses on changes in LTS. This simple metric represents an aggregated risk factor because it neglects age-dependent immunity acquisition associated with transmission intensity. Increases in impacts associated with transitions from malaria-free to epidemic conditions are also not considered.

Hotspots Method. GMT is calculated from the GCM data and change is measured with respect to the reference period 1980–2010. The GMT level in the reference period is ∼0.7 °C above preindustrial, based on estimates for 1980–1999 of 0.51 °C and the average of the five GCMs in ISI-MIP (20). Simulations are binned in temperature bins at ΔGMT = 1 °C, 2 °C, 3 °C, and 4 °C (±0.5 °C). For GIM-GCM combinations where the threshold has not been crossed by ΔGMT = 4.5 °C (the highest temperature bin achieved by GCMs in this study), a value of 5 is assigned. Consequently, cells with a median sectoral crossing temperature above 4.5 °C are not included in the analysis, effectively excluding cells with less than 50% agreement of GIM-GCM combinations on the crossing of the respective threshold. See *SI Text* for more details on the sensitivities and uncertainties of the method. If a grid cell is identified as having crossed the threshold, the whole area of the grid-

cell is assumed to be affected. This process neglects, for example, the separation of agricultural and natural vegetation areas in a grid-cell, which is below the resolution of the analysis. The spread across GIMs is calculated by taking the median over all GCMs for each GIM. The corresponding procedure is used for GCMs.

ACKNOWLEDGMENTS. We thank the anonymous referees for detailed and valuable comments greatly improving this paper; the World Climate Research Programme's Working Group on Coupled Modelling, which is responsible for Coupled Model Intercomparison Project; and the climate modeling groups for producing and making available their model output. The Intersectoral Impact Model Intercomparison Project Fast Track project underlying the framework of this paper was funded by the German Federal Ministry of Education and Research (01LS1201A). For the Coupled Model Intercomparison Project, the US Department of Energy's Program for Climate Model Diagnosis and Intercomparison provides coordinating support and led development of software infrastructure in partnership with the Global Organization for Earth System Science Portals. This study was funded in part by the European Framework Programme FP7/20072013 under Grants 266992 (to F.P.) and 238366 (to A.F.); Joint Department of Energy and Climate Change/Defra Met Office Hadley Centre Climate Programme GA01101 (to D.H.); the Federal Ministry for the Environment (K.F.); the Nature Conservation and Nuclear Safety 11_II_093_Global_A_SIDS_and_LDCs (to K.F.); EUFP7 Quantifying Weather and Climate Impacts on Health in Developing Countries (QWeCI) and HEALTHY FUTURES projects (F.d.J.C.G.); and the Environment Research and Technology Development Fund (S-10) of the Ministry of the Environment, Japan (to Y.M. and K. Nishina).

1. Warren R (2011) The role of interactions in a world implementing adaptation and mitigation solutions to climate change. *Phil Trans R Soc A Math Phys Eng Sci* 369(1934): 217–241.
2. Yohe G, et al. (2006) Global distributions of vulnerability to climate change. *The Integrated Assessment Journal* 6(3):35–44.
3. Fraser EDG, Simelton E, Termansen M, Gosling SN, South A (2013) "Vulnerability hotspots": Integrating socio-economic and hydrological models to identify where cereal production may decline in the future due to climate change induced drought. *Agric For Meteorol* 170:195–205.
4. Giorgi F (2006) Climate change hot-spots. *Geophys Res Lett* 33(8):L08707.
5. Baettig MB, et al. (2007) A climate change index: Where climate change may be most prominent in the 21st century. *Geophys Res Lett* 34(1):L01705.
6. Diffenbaugh NS, Giorgi F (2012) Climate change hotspots in the CMIP5 global climate model ensemble. *Clim Change* 114(3-4):813–822.
7. Patz JA, Kovats RS (2002) Hotspots in climate change and human health. *BMJ* 325(7372):1094–1098.
8. Warszawski L, ISI-MIP Team (2013) The Intersectoral Impact Model Intercomparison Project (ISI-MIP): Project framework description. *Proc Natl Acad Sci USA*, this issue.
9. Meinshausen M, et al. (2009) Greenhouse-gas emission targets for limiting global warming to 2 °C. *Nature* 458(7242):1158–1162.
10. UNFCCC (2009) Report of the Conference of the Parties on its Fifteenth session, and Addendum Part Two: Decisions adopted by the Conference of the parties. Copenhagen, Denmark, December 7–19, 2009.
11. Sachs J, Malaney P (2002) The economic and social burden of malaria. *Nature* 415(6872):680–685.
12. Portmann FT, Siebert S, Döll P (2010) MIRCA2000-global monthly irrigated and rainfed crop areas around the year 2000: A new high-resolution data set for agricultural and hydrological modeling. *Global Biogeochem Cycles* 24(1):GB1011.
13. Heyder U, Schaphoff S, Gerten D, Lucht W (2011) Risk of severe climate change impact on the terrestrial biosphere. *Environ Res Lett* . 10.1088/1748-9326/6/3/034036.
14. Mortimore M (2010) Adapting to drought in the Sahel: Lessons for climate change. *WIREs Clim Change* 1(1):134–143.
15. Warszawski L, et al. (2013) A multi-model analysis of risk of ecosystem shift under climate change. *Proc Natl Acad Sci USA*, this issue.
16. Folke C, et al. (2004) Regime shifts, resilience, and biodiversity in ecosystem management. *Annu Rev Ecol Evol Syst* 35:557–581.
17. Kumar P (2010) *The Economics of Ecosystems and Biodiversity: Ecological and Economic Foundations* (Earthscan, London, Washington).
18. Van Vuuren DP, et al. (2011) The representative concentration pathways: An overview. *Clim Change* 109:5–31.
19. Peters GP, et al. (2013) The challenge to keep global warming below 2 °C. *Nature Climate Change* 3(3):4–6.
20. Brohan P, Kennedy J, Harris I, Tett S, Jones P (2006) Uncertainty estimates in regional and observed temperature changes: A new data set from 1850. *J Geophys Res-Atmos* 111(D12):106–127.
21. Schewe J, et al. (2013) Multi-model assessment of water scarcity under climate change. *Proc Natl Acad Sci USA*, this issue.
22. Rosenzweig C, et al. (2013) Assessing agricultural risks of climate change in the 21st century: A global gridded crop model intercomparison. *Proc Natl Acad Sci USA*, this issue.
23. Deryng D, et al. (2013) Disentangling uncertainties in future crop water productivity under climate change. *Proc Natl Acad Sci USA*, this issue.
24. Kovats RS, et al. (2013) Modelling the impact of climate change on malaria: A comparison of global malaria models. *Proc Natl Acad Sci USA*, this issue.
25. Chaves LF, Koenraadt CJM (2010) Climate change and highland malaria: Fresh air for a hot debate. *Q Rev Biol* 85(1):27–55.
26. Hirabayashi Y, Kanae S, Emori S, Oki T, Kimoto M (2008) Global projections of changing risks of floods and droughts in a changing climate. *Hydrol Sci J* 53(4): 754–772.
27. Hagemann S, et al. (2013) Climate change impact on available water resources obtained using multiple global climate and hydrology models. *Earth Syst. Dynam.* 4(1): 129–144.
28. Frieler K, et al. (2013) The Adaptation Dilemma Caused by Impacts Modeling Uncertainty. *Proc Natl Acad Sci USA*, this issue.
29. Béguin A, et al. (2011) The opposing effects of climate change and socio-economic development on the global distribution of malaria. *Glob Environ Change* 21(4): 1209–1214.
30. Elliott J, et al. (2013) Constraints and potentials of future irrigation water availability on global agricultural production under climate change. *Proc Natl Acad Sci USA*, this issue.
31. Chen C, Haerter JO, Hagemann S, Piani C (2011) On the contribution of statistical bias correction to the uncertainty in the projected hydrological cycle. *Geophys Res Lett* 38(20):L20403.
32. Hempel S, Frieler K, Warszawski L, Schewe J, Piontek F (2013) A trend-preserving bias correction—The ISI-MIP approach. *Earth Syst Dynam Discuss* 4:49–92.
33. Hagemann S, et al. (2011) Impact of a statistical bias correction on the projected hydrological changes obtained from three GCMs and two hydrological models. *J Hydrometeorol* 12(4):556–578.
34. Ehret U, Zehe E, Wulfmeyer V, Warrach-Sagi K, Liebert J (2012) Should we apply bias correction to global and regional climate model data? *Hydrol Earth Syst Sci Discuss* 9: 5355–5387.
35. van Vuuren DP, et al. (2012) A proposal for a new scenario framework to support research and assessment in different climate research communities. *Glob Environ Change* 22(1):21–35.
36. UNDESA (2010) *World Population Prospects, the 2010 Revision* (UNDESA, New York).
37. Rosenzweig C, et al. (2012) The Agricultural Model Intercomparison and Improvement Project (AgMIP): Protocols and pilot studies. *Agric For Meteorol*, 170:166–182.
38. Von Bloh W, Rost S, Gerten D (2010) Efficient parallelization of a dynamic global vegetation model with river routing. *Environmental Modeling* 25(6):685–690.
39. Wirsenius S (2000) *Human Use of Land and Organic Materials* (Chalmers Univ of Technology and Göteborg University, Gothenburg, Sweden).
40. FAO (2001) *Food Balance Sheets: A Handbook* (FAO, Rome).